DOI: 10.1002/chem.200500723

Effect of Alkali Metal Coordination on Gas-Phase Chemistry of the Diphosphate Ion: The $MH_2P_2O_7^-$ Ions

Federico Pepi,[a] Andreina Ricci,*[a] Marzio Rosi,[b] and Marco Di Stefano[b]

Abstract: Systematic experimental and theoretical studies on anionic phosphate species in the gas phase are almost nonexistent, even though they could provide a benchmark for enhanced comprehension of their liquid-phase chemical behavior. Gaseous $MH_2P_2O_7^-$ ions (M = Li, Na, K, Rb, Cs), obtained from electrospray ionization of solutions containing $H_4P_2O_7$ and MOH or M salts as a source of M^+ ions were structurally assayed by collisionally activated dissociation (CAD) mass spectrometry and theoretical calculations at the B3LYP/6-31+G* level of theory. The joint application of mass spectrometric techniques and theoretical methods allowed the $MH_2P_2O_7^-$ ions to be identified as having a structure in which the linear diphosphate anion is coordinated to the M^+ ion (**I**) and provides information on gas-phase isomerization processes in the $[PO_3\cdots MH_2PO_4]^-$ clusters **II** and the $[P_2O_6\cdots M\cdots H_2O]^-$ clusters **IV**. Studies of gas-phase reactivity by Fourier transform ion cyclotron resonance (FTICR) and triple quadrupole (TQ) mass spectrometry revealed that the $MH_2P_2O_7^-$ ions react with selected nucleophiles by clustering, proton transfer and addition–elimination mechanisms. The influence of the coordination of alkali metal ions on the chemical behavior of pyrophosphate is discussed.

Keywords: ab initio calculations · alkali metals · anions · gas-phase reactions · mass spectrometry

Introduction

Noncovalent bonds play a critical role in determining the functions of fundamental materials (proteins, nucleic acids, lipids, hormones, etc.) in biological supramolecular systems. It is through these weak interactions that enzymes are able to bind and release their target molecules. The higher the enzymatic affinity for the substrate in the transition state, the greater the enhancement of the biological reaction rate in the presence of an enzyme. Indeed, knowledge of the mechanism is fundamental to understanding how this catalysis is achieved. The rate enhancement of phosphate ester hydrolysis under enzymatic conditions highlights the high proficiency of enzymes catalysing these processes.[1] The enzymatic reactions of phosphate esters frequently require the presence of one or more metal ions in the active site. The mechanism of phosphate ester hydrolysis with metal-ion-assisted catalysis is the subject of a major theoretical and experimental research effort.[2–15]

Experimental studies of the gas-phase ion chemistry of polyphosphate species are almost nonexistent. The only experimental information available on anionic polyphosphate species in the gas phase is related to the free energies of hydration of singly and doubly charged anions,[16] the electron detachment energies of $H_2PO_4^-$, $H_2P_2O_7^{2-}$, and $H_3P_3O_{10}^{2-}$ [17] and the qualitative and quantitative analysis of inorganic polyphosphates[18] and their esters[19] by mass spectrometric techniques. The only study on gas-phase reactivity focussed on trimethylphosphate and the conjugate base of dimethyl methylphosphonate $(CH_3O)_2P(O)CH_2^-$, which was examined by the flowing afterglow technique.[20]

Recently,[21] ESI ionization was used to examine the behavior of anionic and cationic triphosphate clusters with substances such as choline, acetylcholine, betaine and some peptides. Collisional activation of clusters can be used to induce kinetically forbidden or endothermic reactions between cluster components provided the cluster dissociation

[a] Prof. F. Pepi, Prof. A. Ricci
Dip.to di Studi di Chimica e Tecnologia delle Sostanze Biologicamente Attive
Università di Roma "La Sapienza"
P. le A. Moro 5, 00185 Rome (Italy)
Fax: (+39) 064-991-3602
E-mail: andreina.ricci@uniroma1.it

[b] Prof. M. Rosi, Dr. M. Di Stefano
Istituto di Scienze e Tecnologie Molecolari del CN
c/o Dipartimento di Chimica
Università di Perugia
Via Elce di Sotto 8, 06123 Perugia (Italy)

energy is sufficiently high. In some cases, phosphorylation of a hydroxy group is observed.

Theoretical studies, aimed at elucidating the mechanism of pyrophosphate hydrolysis, first considered equilibrium structures, the enthalpy of the hydrolysis reaction[22,23] and the influence of hydration.[24] The gas-phase hydrolysis reaction was found to be endothermic for the monoanion, $H_3P_2O_7^-$, and highly exothermic for the di- and trianions, $H_2P_2O_7^{2-}$ and $HP_2O_7^{3-}$.[15,23] Evaluations of the heat of gas-phase hydrolysis that take into account metal-ion coordination of the pyrophosphate anion were first accomplished for alkali metal cations[15b] and subsequently extended to metal dications such as Ca^{2+}, Mg^{2+}, and Zn^{2+}.[11–15]

Coordination of Mg^{2+} elongates one of the P–O bridging bonds in the $[MgH_nP_2O_7]^{(2-n)-}$ ions ($n=0,1,2$) and plays a catalytic role in their isomerization to $[H_nPO_4\cdots Mg\cdots PO_3]^{(2-n)-}$. The gas-phase isomerization energies of the $[MgH_nP_2O_7]^{(2-n)-}$ ($n=1, 2$) and $[CaH_nP_2O_7]^{(2-n)-}$ ($n=0, 1, 2$) species were computed.[13,14] The $[MH_nP_2O_7]^{(2-n)-}\rightarrow [H_nPO_4\cdots M\cdots PO_3]^{(2-n)-}$ processes ($n=0, 1, 2$; M = Mg, Ca, Zn) were also studied in the presence of a water molecule, and the role played by the metal cation was investigated.[11,12]

Systematic experimental and theoretical gas-phase studies on isolated anionic phosphate species are valuable for the purpose of obtaining information about their intrinsic properties and providing a benchmark for enhanced comprehension of their liquid-phase chemistry.

Furthermore, understanding the effects of solvation and metal–cation coordination, of increasing chain length and charge, could prove useful for comprehending structural and energetic factors that stabilize the phosphate transition state in the active sites of enzymes.

Recently, we reported a systematic study of the gas-phase ion chemistry of the diphosphate anion $H_3P_2O_7^-$.[25] This investigation was subsequently extended to the $H_5P_2O_8^-$ ions to evaluate the role of the first water molecule of hydration and to gain insight into the gas-phase mechanism of the hydrolysis and synthesis of the pyrophosphate anion.[26]

The present work evaluates the influence of coordination with alkali metal cations on the gas-phase chemistry of the diphosphate anion ion and addresses the structure, stability and reactivity of $MH_2P_2O_7^-$ (M = Li, Na, K, Rb, Cs) anions. The first preparation and structural characterization of gaseous $MH_2P_2O_7^-$ ions, by the joint application of mass spectrometric techniques such as electrospray ionization Fourier transform ion cyclotron resonance (ESI-FTICR-MS) and triple quadrupole mass spectrometry (ESI-TQ-MS) and theoretical methods, is described.

Results

Generation of gaseous $MH_2P_2O_7^-$ ions: The $MH_2P_2O_7^-$ ions (M = Li, Na, K, Rb, Cs) were formed by electrospray ionization of 10^{-4} M solutions containing $H_4P_2O_7$ and MOH bases or M salts as a source of M^+ ions in CH_3CN/H_2O (1/1). By way of example we report the ESI spectra of solutions containing $H_4P_2O_7$ and $LiClO_4$ (Figure 1a) or NaOH (Figure 1b). High $NaH_2P_2O_7^-$ ion intensity was also obtained by dissolving $Na_4P_2O_7$ in CH_3CN/H_2O (1/1) or CH_3OH/H_2O (1/1) solutions. The $MH_2P_2O_7^-$ ions were never detected in the ESI spectra of solutions containing H_3PO_4 and MOH or M salts.

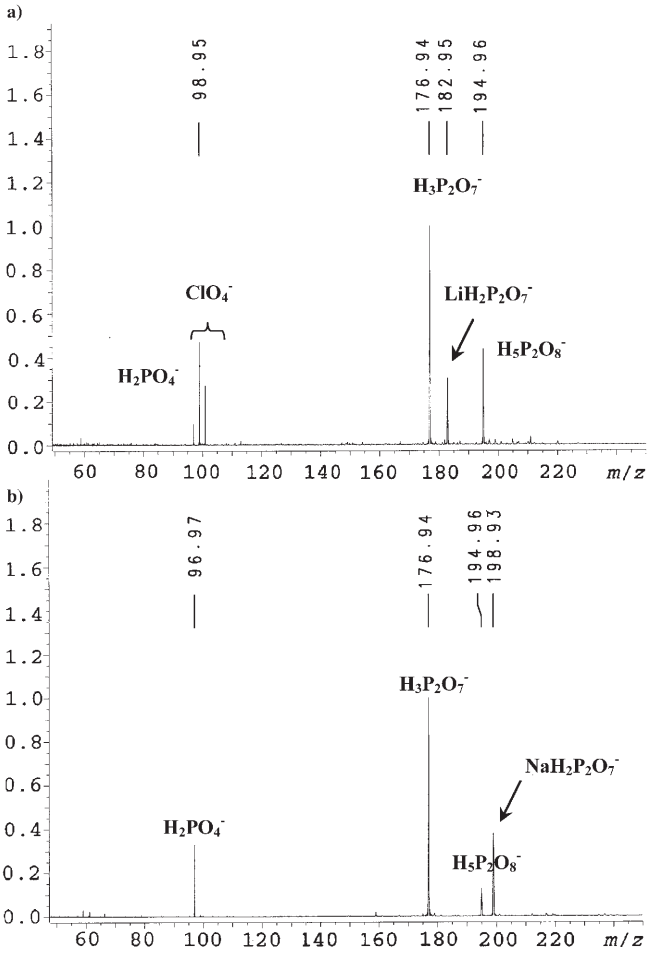

Figure 1. a) ESI spectrum of CH_3CN/H_2O (1/1) solution of $H_4P_2O_7$ and $LiClO_4$ (1/1). b) ESI spectrum of CH_3CN/H_2O (1/1) solution of $H_4P_2O_7$ and NaOH (1/1).

ESI-FTICR mass spectrometric experiments

Structural characterization of $MH_2P_2O_7^-$ ions: The $MH_2P_2O_7^-$ ions generated in the external ESI source of the FTICR mass spectrometer were isolated in the resonance cell and allowed to undergo collisionally activated decomposition (CAD). The CAD spectra of all the $MH_2P_2O_7^-$ ions display a fragment at m/z 79 corresponding to the PO_3^- ion. A second minor fragmentation channel corresponding to the loss of a water molecule was observed for the $LiH_2P_2O_7^-$ ion.

Reactivity of $MH_2P_2O_7^-$ ions: The $MH_2P_2O_7^-$ ions isolated and thermalized in the FTICR cell by collisions with Ar, introduced through a pulse valve, were allowed to react with neutral species. Table 1 lists the compounds used to investigate the gas-phase reactivity of $MH_2P_2O_7^-$ ions, their gas-phase acidities, the observed reactions and the molecular formula of the products.

Table 1. Gas-phase reactivity of $MH_2P_2O_7^-$ ions by FTICR mass spectrometry.

Compound	ΔH°_{acid} [kcal mol^{-1}]	Reaction[a]	Products
H_2O	390.7	–	–
CH_3OH	382.0	–	–
CH_3CH_2OH	378.3	–	–
CH_3COCH_3	367.6	–	–
CF_3CH_2OH	361.7	CL	$[CF_3CH_2OH,MH_2P_2O_7]^-$
CF_3COCH_3	349.2	–	–
$(CF_3)_2CHOH$	345.0	CL	$[(CF_3)_2CHOH,MH_2P_2O_7]^-$
CF_3COOH	323.8	PT, CL	CF_3COO^-, $H_3P_2O_7^-$, $[CF_3COOH,MH_2P_2O_7]^-$
$(CH_3)_3SiN_3$	(HN_3) 343,9	AE	$[(CH_3)_3Si,MHP_2O_7]^-$, $[2(CH_3)_3Si,MP_2O_7]^-$

[a] AE = addition/elimination, CL = clustering, PT = proton transfer.

Under the low-pressure conditions of the FTICR experiments (10^{-7}–10^{-8} mbar), the $MH_2P_2O_7^-$ ions are inert toward H_2O, CH_3OH, C_2H_5OH and CH_3COCH_3. Their reaction with CF_3CH_2OH and $(CF_3)_2CHOH$ leads to the formation of ionic products corresponding to addition of the alcohol molecule. The rate constants of adduct formation are significantly higher for $(CF_3)_2CHOH$ (ca. 2.0×10^{-10} molecules cm^3 s^{-1}) than for CF_3CH_2OH (ca. 3.0×10^{-11} molecules cm^3 s^{-1}), but in both cases increase slightly on going from $LiH_2P_2O_7^-$ to $NaH_2P_2O_7^-$ and become almost constant for $RbH_2P_2O_7^-$ and $CsH_2P_2O_7^-$. No reaction was observed between the $MH_2P_2O_7^-$ ions and CF_3COCH_3.

A typical time profile of the ion intensities of the reaction between $NaH_2P_2O_7^-$ and CF_3COOH is shown in Figure 2. The reaction of $MH_2P_2O_7^-$ ions with CF_3COOH yields $H_3P_2O_7^-$ ions at *m*/*z* 177 as the main ionic product, except for M = Li. Furthermore, proton transfer from trifluoroacetic acid to the more basic $MH_2P_2O_7^-$ anions, which leads to formation of the CF_3COO^- ions at *m*/*z* 113, is always observed. The ratio of the $H_3P_2O_7^-/CF_3COO^-$ ion intensities increases on going from Li to Rb. The $[CF_3COOH,MH_2P_2O_7]^-$ addition products are detected only in the reactions involving $LiH_2P_2O_7^-$ and $NaH_2P_2O_7^-$ions.

Ionic products corresponding to the addition of one or two molecules of $SiMe_3N_3$ followed by the loss of one or two HN_3 moieties are detected when the $MH_2P_2O_7^-$ ions react with $Si(CH_3)_3N_3$.

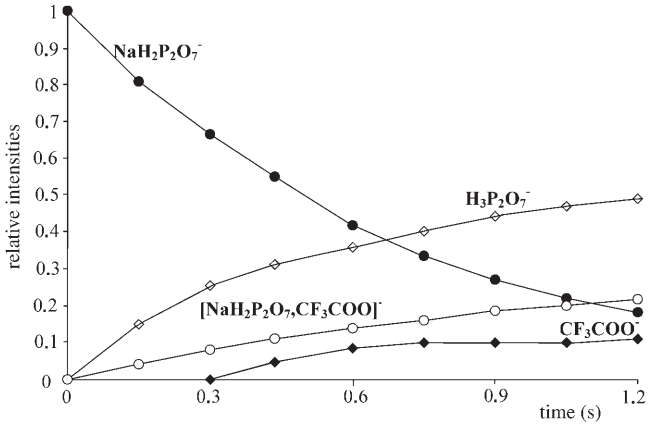

Figure 2. FTICR time profile of the ion intensities for the reaction between $NaH_2P_2O_7^-$ ions and CF_3COOH at a pressure of 4.5×10^{-8} mbar.

ESI-TQ mass spectrometric experiments

Structural characterization of $MH_2P_2O_7^-$ ions: The CAD spectra of the $MH_2P_2O_7^-$ (M = Li, Na, K) ions display two characteristic fragmentation channels corresponding to the loss of a water molecule and of the MH_2PO_4 moiety. The energy-resolved TQ-CAD spectrum of the $LiH_2P_2O_7^-$ ion at *m*/*z* 183, recorded at nominal centre-of-mass collision energies ranging from 0 to 4.5 eV, is shown in Figure 3.

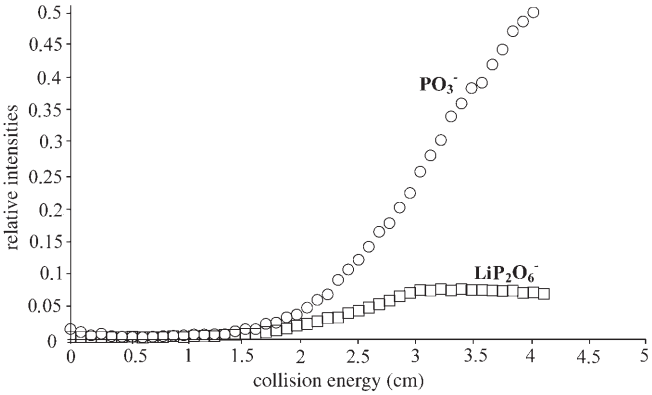

Figure 3. Energy-resolved TQ-CAD spectrum of $LiH_2P_2O_7^-$ ions.

It shows the characteristic fragmentation into the $LiP_2O_6^-$ ion at *m*/*z* 165, corresponding to the loss of a water molecule, and into the PO_3^- ion at *m*/*z* 79, corresponding to the loss of LiH_2PO_4. The loss of the water molecule occurs at slightly higher energy than is required for the loss of the LiH_2PO_4 moiety. Figure 4 shows the energy-resolved CAD spectra of all the $MH_2P_2O_7^-$ ions with the profiles of relative intensities of the fragments arising from the loss of H_2O (b) and of the fragment at *m*/*z* 79 resulting from the loss of MH_2PO_4 (a). The CAD spectra of the $RbH_2P_2O_7^-$ and $CsH_2P_2O_7^-$ ions display only the PO_3^- fragment ion.

Loss of a water molecule occurs at comparable energies for Li, Na and K, although the $MP_2O_6^-$ ion intensities de-

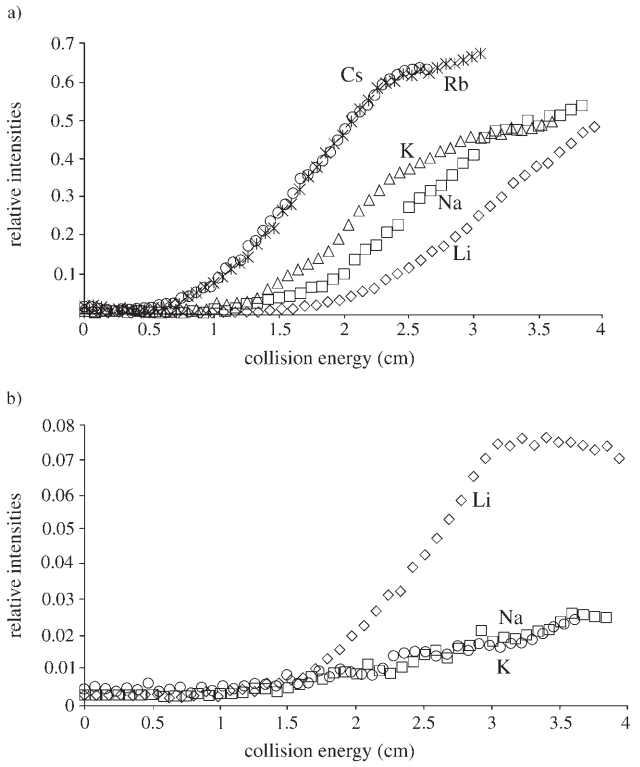

Figure 4. Energy-resolved CAD spectra of the $MH_2P_2O_7^-$ anions showing the intensity profile of the fragment at *m*/*z* 79 resulting from the loss of MH_2PO_4 (a) and the intensity profile of the fragment arising from the loss of H_2O (b).

crease on going from Li to K. Conversely, formation of the PO_3^- fragment is strongly influenced by the nature of the cation involved; it occurs at lower collision energies with decreasing charge-to-radius ratio of the cation. Finally, in the CAD spectra of all the $MH_2P_2O_7^-$ ions, traces (<4% of precursor ion intensity) of the $H_2PO_4^-$ fragment ion at *m*/*z* 97 were detected for centre-of-mass collision energies higher than 3.0 eV.

Reactivity of the $MH_2P_2O_7^-$ ions: Two kinds of experiments were performed by TQ mass spectrometry to investigate the reactivity of the $MH_2P_2O_7^-$ ions.

First, the $MH_2P_2O_7^-$ anions, mass-selected by the first quadrupole, were allowed to react in the collision cell with neutral substrates at collision energies ranging from 0 to 10 eV (laboratory frame).

The reaction between the $MH_2P_2O_7^-$ ions (M=Li, Na, Rb) and CF_3COOH leads to the formation of addition products that, when excited by the exothermicity of the formation process and by the increasing translational energy of the impinging ion, dissociate into CH_3COO^- and $H_3P_2O_7^-$ fragments at *m*/*z* 113 and *m*/*z* 177, respectively. The ratio of the $H_3P_2O_7^-/CF_3COO^-$ ion intensities increases on passing from Li to Rb. The ion at *m*/*z* 177 becomes the predominant dissociation channel of the addition product containing the Rb cation.

Clustering is not observed when alcohols such as CH_3OH and C_2H_5OH are introduced into the cell, but occurs when the $MH_2P_2O_7^-$ ions are allowed to react with CF_3CH_2OH and $(CF_3)_2CHOH$. Increasing the kinetic energy of the $MH_2P_2O_7^-$ ions induces cluster backdissociation. Small amounts (<1%) of the PO_3^-, $MP_2O_6^-$ and $H_2PO_4^-$ fragment ions were also observed in the investigated range of low collision energies. The intensities of the $[CF_3CH_2OH,MH_2P_2O_7^-]$ and $[(CF_3)_2CHOH,MH_2P_2O_7^-]$ ions increase on going from Li to Rb.

In a second type of TQ-MS experiment, we tried to prepare the $[MH_2P_2O_7,alcohol]^-$ adducts directly in the ESI source by adding alcohols such as CH_3OH, C_2H_5OH, CF_3CH_2OH and $(CF_3)_2CHOH$ to the $H_4P_2O_7/M^+$ solutions. Clusters with the $MH_2P_2O_7^-$ ions were formed exclusively in the case of trifluoroethyl and hexafluoroisopropyl alcohols. These adducts were mass-selected by the first quadrupole and allowed to undergo collisionally activated dissociation in the cell. These clusters were found essentially to backdissociate. Also in this case small amounts of the PO_3^-, $MP_2O_6^-$ and $H_2PO_4^-$ ions were observed. In particular, the last-named species appears at a centre-of-mass collision energy of about 1 eV, considerably lower than that observed in the CAD spectra of the $MH_2P_2O_7^-$ ions, although its intensity remains very low (< 1% of precursor ion).

Theoretical results: To gain information on the structure of the $MH_2P_2O_7^-$ ions investigated by mass spectrometric techniques we performed a systematic theoretical study at the B3LYP level of theory. The study of the $MH_2P_2O_7^-$ potential energy surfaces led to the characterization of numerous structural isomers of the species of interest. In agreement with the experimental evidence, four different groups of anions **I**–**IV** were optimized.

$[H_2P_2O_7\cdots M]^-$ **I** $[H_2PO_4\cdots M\cdots PO_3]^-$ **II**

$[PO_3\cdots M\cdots PO_3\cdots H_2O]^-$ **III** $[H_2O\cdots M\cdots P_2O_6]^-$ **IV**

A letter following the group number indicates the coordinated metal ion (**a**=Li, **b**=Na, **c**=K, **d**=Rb, **e**=Cs). For each isomer, only structures corresponding to true minima are reported.

In ions of group **I**, linear $H_2P_2O_7^{2-}$ ions are coordinated to the M^+ cation. The ions of groups **II** and **III** are characterized by a cluster structure in which the M^+ cation holds together the PO_3^- and the $H_2PO_4^-$ anions (group **II**), or the PO_3^- and the $[PO_3\cdots H_2O]^-$ moieties (group **III**). Ions of group **IV** are characterized by the presence of the dimetaphosphate anion and a water molecule, electrostatically bound to the M^+ cation.

We optimized the structures of $MH_2P_2O_7^-$ and MH_2PO_4 for the whole alkali metal group. As the differences in the optimized structures are not particularly significant, we restrict the theoretical analysis to Li and Na.

Tables 2 and 3 list the dissociation energies and thermochemical parameters of the isomerization processes of the investigated species containing the Li^+ and Na^+ cations, respectively, computed at the B3LYP/6-31+G* level of theory.

Table 2. Isomerization and dissociation energies [kcal mol^{-1}] of the investigated processes for $LiH_2P_2O_7^-$ at the B3LYP/6-31+G* level of theory.

Reaction	ΔH	E_a
Ia→**IVa**	13.8	47.1
Ia→**IIa**	12.6	41.2
IIa→**IIIa**	17.4	35.7
IVa→$LiP_2O_6^- + H_2O$	25.4	–
IIa→$LiH_2PO_4 + PO_3^-$	−16.5	–
IIIa→$[PO_3\cdots Li\cdots PO_3]^- + H_2O$	11.5	–

Table 3. Isomerization and dissociation energies [kcal mol^{-1}] of the investigated processes for $NaH_2P_2O_7^-$ at the B3LYP/6-31+G* level of theory.

Reaction	ΔH	E_a
Ib→**IVb**	9.9	42.8
Ib→**IIb**	5.2	31.2
IIb→**IIIb**	17.0	34.0
IVb→$NaP_2O_6^- + H_2O$	12.8	–
IIb→$NaH_2PO_4 + PO_3^-$	−20.1	–
IIIb→$[PO_3\cdots Na\cdots PO_3]^- + H_2O$	10.2	–

The $[H_2P_2O_7\cdots M]^-$ clusters (group I): Figure 5 shows the optimized geometries at the B3LYP/6-31+G* level of theory of the ions **I** formed by electrostatic interaction of the linear $H_2P_2O_7^{2-}$ ion and M^+ cations. The stationary geometries found for all $MH_2P_2O_7^-$ ions (M = Li, Na, K, Rb, Cs) **Ia**–**Ie**, are in good agreement with those previously reported.[15b] The alkali metal cations are coordinated to the diphosphate ion by two oxygen atoms belonging to two different phosphate units. With decreasing charge-to-radius ratio of the metal cation, the M–O bond length and the P-O-P angle increase. However, the M–O bond lengths are always shorter than those of MH_2PO_4, the geometries of which are shown in Figure 6. An intramolecular hydrogen bond stabilizes the eclipsed configurations **Ia**–**Ie**. The presence of one hydrogen atom in both phosphate subunits and the symmetry of electrostatic interaction induced by the cation do not produce the elongation of one bridging P-O-P bond with respect to the other, as occurs in the staggered configurations of $ZnH_2P_2O_7$, $CaH_2P_2O_7$ and $MgH_2P_2O_7$ species.[11]

The $[H_2PO_4\cdots M\cdots PO_3]^-$ clusters (group II): Figure 7 displays the optimized geometries at the B3LYP/6-31+G* level of theory of clusters **II** in which $H_2PO_4^-$ and PO_3^- ions are held together by the M^+ cation. In the stationary geometries found for **IIa** and **IIb**, the metal cation is coordinated to the metaphosphate group by one oxygen atom and to the orthophosphate group by two proton-free oxygen atoms. The O–M bond lengths are slightly longer for Na than for Li.

As reported in Tables 2 and 3, the dissociation of clusters **IIa** and **IIb** into the PO_3^- ion and LiH_2PO_4 or NaH_2PO_4 is

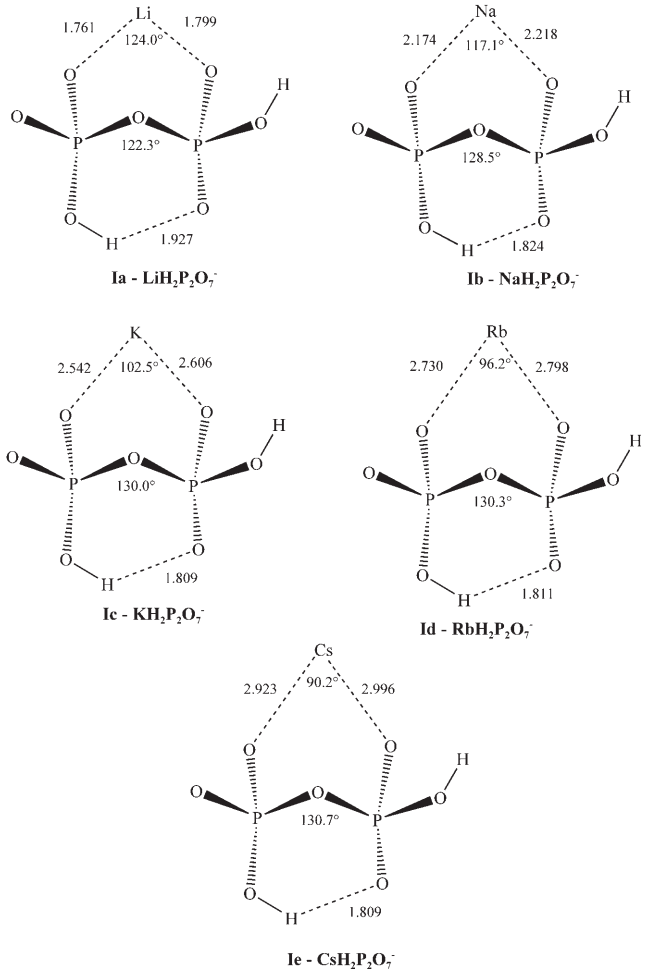

Figure 5. Optimized geometry at the B3LYP/6-31+G* level of theory of the $MH_2P_2O_7^-$ anions (group **I**). Bond lengths in Å and angles in degrees.

exothermic by 16.5 and 20.1 kcal mol^{-1}, respectively, at our level of theory. This result characterizes these species as unstable intermediates in the gas phase, liable to decompose into the PO_3^- and MH_2PO_4 moieties once formed by isomerization of **I** (vide infra). Isomerization of $[H_2P_2O_7\cdots M]^-$ ions **I** to the $[H_2PO_4\cdots M\cdots PO_3]^-$ ions **II**, the energetic profile of which is illustrated in Figures 8 and 9, is an important pathway since, in principle, reactions involving diphosphate anions that result in hydrolysis or transfer of the phosphoryl group can occur through a dissociative mechanism, in analogy to phosphate monoesters. The simplest gas-phase reaction mechanism leading to dissociation of the $MH_2P_2O_7^-$ anion into PO_3^- and $H_2PO_4^-$ ions coordinated to the metal cation involves intramolecular proton transfer via a four-membered transition state. However, the critical step seems to be transfer of a hydrogen atom from the oxygen atom coordinated to the metal to the other oxygen atom, as can be seen from the geometry of the transition states reported in Figures 10 and Figure 11. The isomerization of **Ia** to **IIa** was computed to be endothermic by 12.6 kcal mol^{-1} with a energy barrier of 41.2 kcal mol^{-1} at the B3LYP/6-31+G* level of theory. The endothermicity and barrier height of the

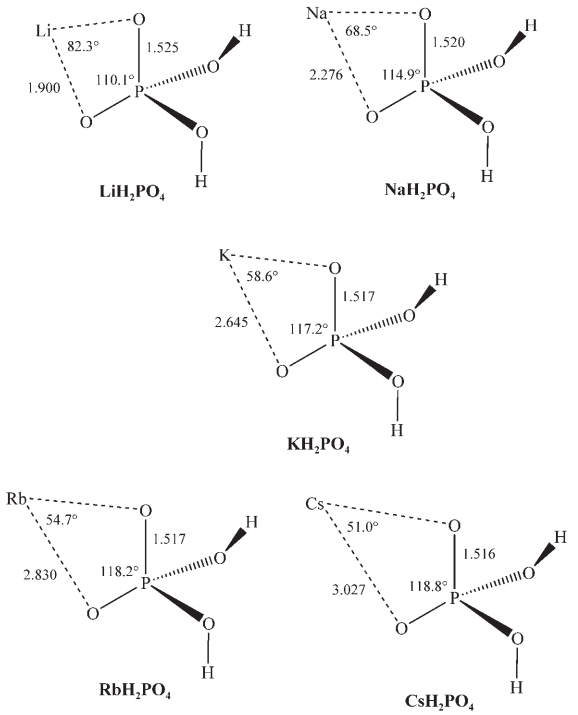

Figure 6. Optimized geometries at B3LYP/6-31+G* level of theory of MH_2PO_4. Bond lengths in Å and angles in degrees.

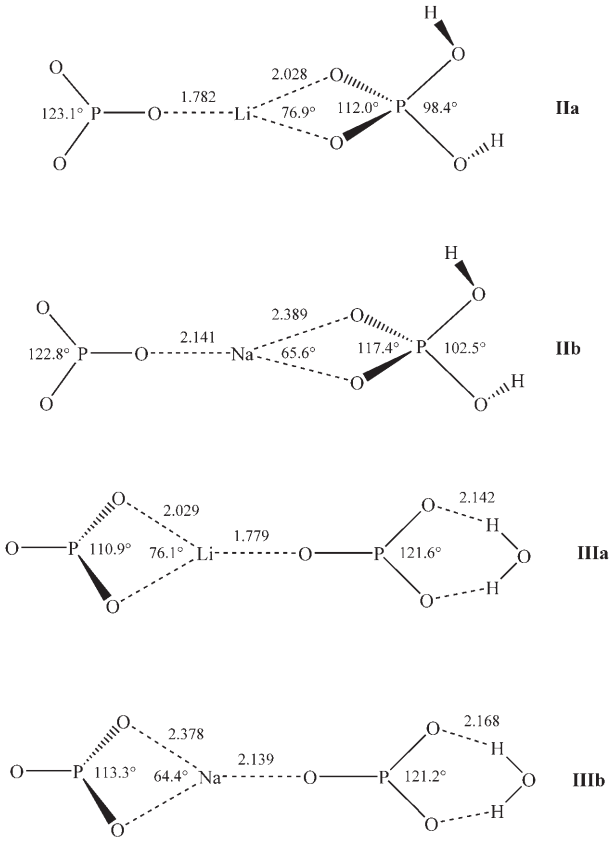

Figure 7. Optimized geometries at B3LYP/6-31+G* level of theory of the $[H_2PO_4\cdots Li\cdots PO_3]^-$ and $[H_2PO_4\cdots Na\cdots PO_3]^-$ clusters (group **II**) and of the $[PO_3\cdots Li\cdots PO_3\cdots H_2O]^-$ and $[PO_3\cdots Na\cdots PO_3\cdots H_2O]^-$ clusters (group **III**). Bond lengths in Å and angles in degrees.

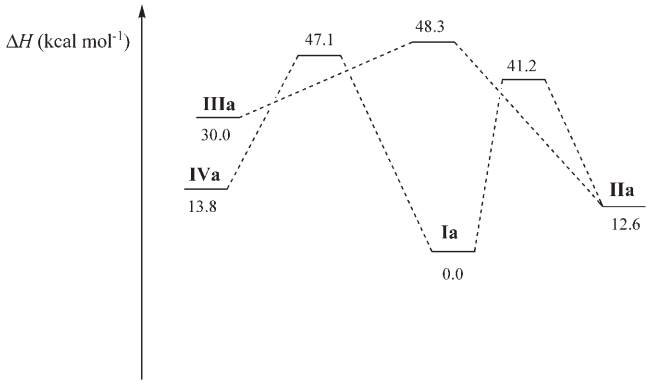

Figure 8. Schematic representation at the B3LYP/6-31+G* level of theory of the isomerization of the $LiH_2P_2O_7^-$ ions. All thermochemical parameters are given in kcal mol^{-1} and were calculated at 298.15 K.

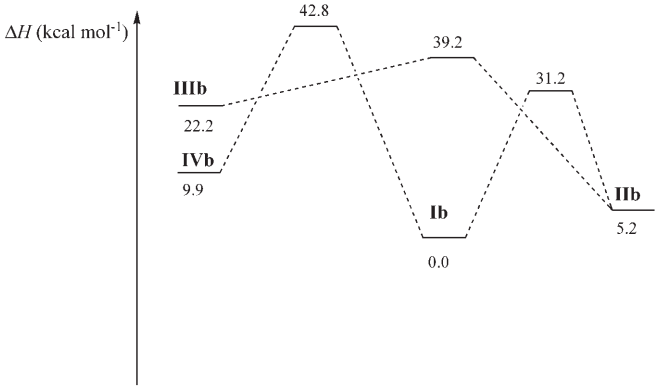

Figure 9. Schematic representation at the B3LYP/6-31+G* level of theory of the isomerization of the $NaH_2P_2O_7^-$ ions. All thermochemical parameters are given in kcal mol^{-1} and were calculated at 298.15 K.

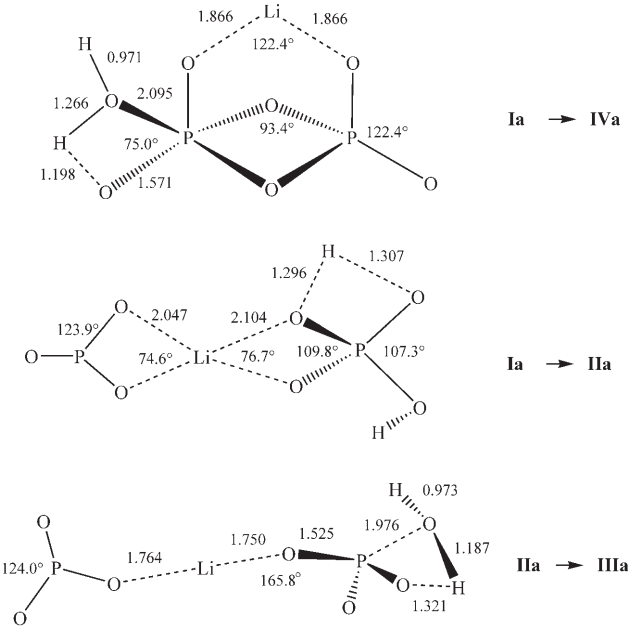

Figure 10. Optimized geometries at B3LYP/6-31+G* level of theory of the transition states involved in the isomerizations of ions **Ia** and **IIa**. Bond lengths in Å and angles in degrees.

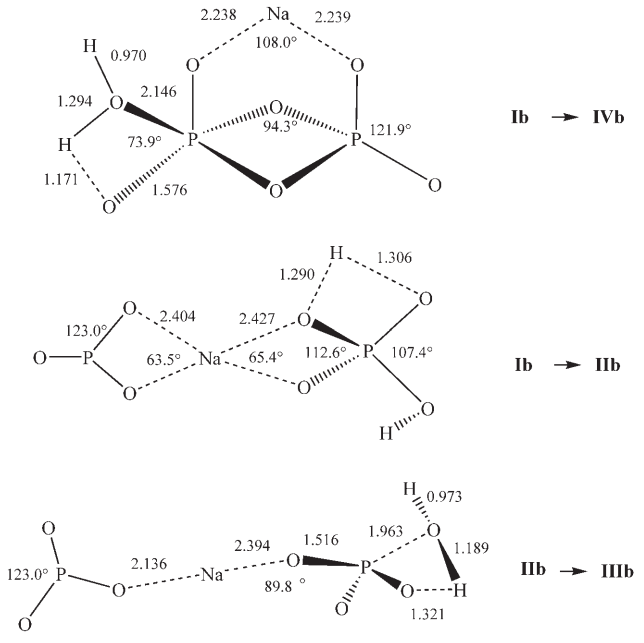

Figure 11. Optimized geometries at the B3LYP/6-31+G* level of theory of the transition states involved in the isomerizations of ions **Ib** and **IIb**. Bond lengths in Å and angles in degrees.

isomerization of **Ib** to **IIb** were calculated to be 5.2 and 31.2 kcal mol^{-1}, respectively.

The $[PO_3\cdots M\cdots PO_3\cdots H_2O]^-$ clusters (group III): Figure 7 shows the optimized geometry at the B3LYP/6-31+G* level of theory of clusters **III**, in which the M^+ cation is electrostatically coordinated to two PO_3^- anions, one of which is coordinated to a water molecule. Dissociation of the $[PO_3\cdots H_2O]^-$ moiety into H_2O and PO_3^- is endothermic by 11.5 and 10.2 kcal mol^{-1} for **IIIa** and **IIIb**, respectively.

All our attempts to optimize the geometry of the cluster $[PO_3\cdots M\cdots H_2O]$ arising from the loss of the PO_3^- ion from **III** were unsuccessful.

Isomerization of the $[H_2PO_4\cdots M\cdots PO_3]^-$ ions **II** to the $[PO_3\cdots M\cdots PO_3\cdots H_2O]^-$ ions **III** is endothermic by 17.4 kcal mol^{-1} with an energy barrier of 35.7 kcal mol^{-1} for M = Li, and endothermic by 17.0 kcal mol^{-1} with an energy barrier of 34.0 kcal mol^{-1} for M = Na. The geometries of the transition states (Figures 10 and 11) shows that the critical step in this case is the transfer of a hydrogen atom from one oxygen atom to the other oxygen atom bound to phosphorus.

The $[H_2O\cdots M\cdots P_2O_6]^-$ clusters (group IV): Under conditions of low collision energy the CAD spectra of $MH_2P_2O_7^-$ ions display the $MP_2O_6^-$ ions, which correspond to the loss of a water molecule. In our previous study on the diphosphate monoanion, we identified two isomeric forms of the $HP_2O_6^-$ anion: a linear structure maintaining the pyrophosphate P-O-P linkage and a second structure characterized by the presence of a four-membered ring in which the P atoms are connected to each other by two O–P bonds. The latter species lies 24.4 kcal mol^{-1} below the former at the CCSD(T)/6-31+G* level of theory.[25,26] In principle, the $[MP_2O_6\cdots H_2O]^-$ ions could be formed from the $MH_2P_2O_7^-$ ions. The optimized geometries of clusters **IVa** and **IVb**, in which the cyclic $LiP_2O_6^-$ and $NaP_2O_6^-$ ions are solvated by a water molecule, are reported in Figure 12. The barrier height for

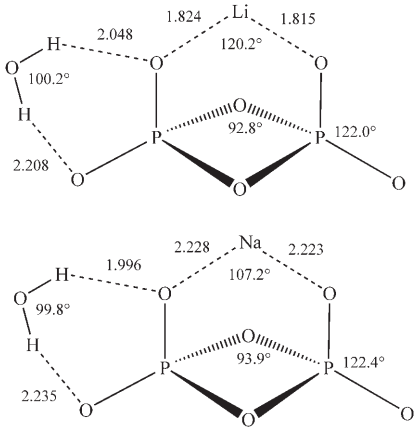

Figure 12. Optimized geometries at the B3LYP/6-31+G* level of theory of the $[MP_2O_6\cdots H_2O]^-$ clusters (group **IV**). Bond lengths in Å and angles in degrees.

the isomerization $MH_2P_2O_7^- \rightarrow [MP_2O_6\cdots H_2O]$ is computed to be 47.1 kcal mol^{-1} for M = Li and 42.8 kcal mol^{-1} for M = Na, while the process is endothermic by 13.8 and 9.9 kcal mol^{-1}, respectively. The geometries of the transition states reported in Figures 10 and 11 show that also in this case the critical step is the transfer of a hydrogen atom. The dissociation of clusters **IVa** and **IVb** into $MP_2O_6^-$ and water is endothermic by 25.4 and 12.8 kcal mol^{-1}, respectively.

Discussion

In the absence of model ions of known connectivity, we can structurally characterize the $MH_2P_2O_7^-$ ions on the basis of energetic considerations.

The energy-resolved CAD mass spectra of $MH_2P_2O_7^-$ ions (M = Li, Na, K) show two characteristic fragmentations corresponding to loss of water and loss of MH_2PO_4 to give $MP_2O_6^-$ and PO_3^- fragment ions, respectively.

The energy profiles depicted in Figures 8 and 9, allow the $[MH_2P_2O_7]^-$ ions **I** to be identified as the species responsible for the formation of both these fragments. In fact, the PO_3^- ion can be formed from the $[MH_2P_2O_7]^-$ ions **I** after isomerization to the $[H_2PO_4\cdots M\cdots PO_3]^-$ clusters **II**, a process requiring 41.2 and 31.2 kcal mol^{-1} for M = Li and M = Na, respectively, and subsequent exothermic dissociation of **II** into PO_3^- and $[H_2PO_4\cdots M]$. The loss of a water molecule from ions **I** occurs by a two-step mechanism requiring isomerization to $[H_2O\cdots M\cdots P_2O_6]^-$ clusters **IV**, a process with a barrier of 47.1 and 42.8 kcal mol^{-1} for M = Li and M = Na, respectively, and subsequent dissociation of cluster **IV** into H_2O

and $[M\cdots P_2O_6]^-$, which is endothermic by 25.4 and 13.0 kcal mol^{-1} for M = Li and M = Na, respectively. The latter process is strongly influenced by the nature of the metal cation, but the dissociation energy is always lower than the energy required for the **I**→**IV** isomerization. Indeed, according to theoretical calculations, the formation of the PO_3^- fragment from ions **I** strongly depends on the nature of the alkali metal cation, whereas the loss of H_2O is scarcely influenced by the nature of M^+.

In accordance with theoretical results, the CAD spectra reported in Figure 4 show that the PO_3^- appearance energies decrease with decreasing charge-to-radius ratio of the metal cation. Conversely, the dissociation energy thresholds for loss of the water molecule are almost unaffected by the different coordinated metal ions, and the intensities of the $MP_2O_6^-$ fragments decrease from M = Li to M = K and disappear completely for $RbH_2P_2O_7^-$ and $CsH_2P_2O_7^-$. This can be rationalized by considering the relative energy difference between the energy barriers of the two fragmentation channels. The loss of MH_2PO_4 is favored more than the loss of the water molecule on going from Li to K, and in the case of $RbH_2P_2O_7^-$ and $CsH_2P_2O_7^-$, facile fragmentation into PO_3^- ions precludes the observation of any other dissociation channel.

The existence of the other isomers can be excluded on the basis of the following considerations. The exothermicity of the barrierless dissociation process of the $[H_2PO_4\cdots M\cdots PO_3]^-$ clusters into the PO_3^- ions characterizes ions **II** as intermediates that are unstable in the gas phase. This process is exothermic for both the Li and the Na cations, and even more favored for the larger alkali metal ions K, Rb, and Cs.

Cluster **III** can lose a water molecule to form the $[PO_3\cdots M\cdots PO_3]^-$ fragment ion, but this dissociation, according to theoretical calculations, requires about 10 kcal mol^{-1}, a dissociation energy undoubtedly lower than that required for the loss of the MH_2PO_4 moiety from ions **I**. Cluster **IV** may also lose a water molecule, but its formation can be excluded, since theoretical calculations show that this process is highly dependent on the nature of M^+.

We can conclude that the gaseous $MH_2P_2O_7^-$ ions generated by electrospray ionization of solutions containing $H_4P_2O_7$ and M^+ cations have the structure of ions **I**.

Additional evidence corroborates the structural characterization of $MH_2P_2O_7^-$ ions. These ions have never been detected in the ESI spectra of solutions containing H_3PO_4 and MOH or M salts. In our previous investigations of the $H_3P_2O_7^-$[25] and $H_5P_2O_8^-$ ions,[26] we hypothesized the existence of mixed isomeric ionic populations containing both covalently bonded and cluster species on the basis of the evidence that these ions were present in the ESI spectra of solutions of both diphosphoric and phosphoric acids and, regardless of their origin, exhibited the same CAD spectra and the same reactivity. The computed dissociation energies of the $[H_3PO_4\cdots PO_3]^-$ and $[H_2PO_4\cdots H_3PO_4]^-$ clusters, which are as high as 30 kcal mol^{-1}, characterize these aggregates as extremely stable in the gas phase and justify the hypothesis of mixed isomeric ionic populations. Probably, in $H_4P_2O_7$ solutions these clusters arise from the hydrolysis of diphosphoric acid. Conversely, in the case of $MH_2P_2O_7^-$ ions, the corresponding $[H_2PO_4\cdots M\cdots PO_3]^-$ clusters are found to be unstable in the gas phase.

The $MH_2P_2O_7^-$ ions react with selected nucleophiles by clustering, proton transfer and addition–elimination mechanisms (Table 1). Clustering and proton transfer reactions are observed under FTICR and TQ conditions with substrates having a gas-phase acidity comparable to that of the $MH_2P_2O_7^-$ ions. The gas-phase acidity of $MH_3P_2O_7$, that is, the proton affinity of the $MH_2P_2O_7^-$ anions, was evaluated at the DZP SCF level of theory as 328 kcal mol^{-1} for the $LiH_2P_2O_7^-$ ion and 336 kcal mol^{-1} for the $NaH_2P_2O_7^-$ ion.[15b] Accordingly, clustering of the $LiH_2P_2O_7^-$ and $NaH_2P_2O_7^-$ ions is observed with CF_3COOH (ΔH°_{acid} = 323.8 kcal mol^{-1}).[27] Probably, at the low pressure of FTICR experiments, the higher exothermicity of proton transfer from CF_3COOH to $KH_2P_2O_7^-$, $RbH_2P_2O_7^-$, and $CsH_2P_2O_7^-$ does not allow stabilization of the addition complex, whereas at the higher pressure of the TQ collision cell, the addition products are observed for all the $MH_2P_2O_7^-$ ions. In addition, the two other products of the reaction, the CF_3COO^- and $H_3P_2O_7^-$ ions, reasonably arise from the decomposition of the addition product following loss of the $MH_3P_2O_7$ and CF_3COOM moieties, respectively. A possible explanation of this reactivity involves the mechanism shown in Scheme 1, the first step of which is formation of an ion–neutral complex **INC1** between the $MH_3P_2O_7^-$ ion and CF_3COOH, in which the alkali metal cation is coordinated with the C=O group and a phosphate oxygen atom is involved in a hydrogen bond. Subsequently, **INC1** can isomerize to **INC2** by a concerted or a stepwise mechanism involving proton transfer.

Indeed, CF_3COO^- and $H_3P_2O_7^-$ can be eliminated by **INC2**. Except for M = Li, the formation of $H_3P_2O_7^-$ is the most favoured channel for all the $MH_2P_2O_7^-$ ions. The $CF_3COO^-/H_3P_2O_7^-$ intensity ratio decreases on going from Li to Rb, and this suggests easier metal exchange from the phosphate to the trifluoroacetate ion owing to the softer

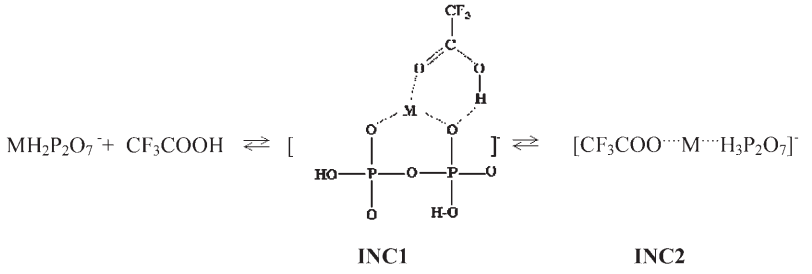

Scheme 1. Hypothetical mechanism for the reaction of $MH_2P_2O_7^-$ ions with CF_3COOH.

character of the metal cation. In the absence of the metal cation, only the addition product was detected, as we reported in our previous study on $H_3P_2O_7^-$ ions.[25]

From tabulated gas-phase acidities,[27] proton transfer from $MH_2P_2O_7^-$ to CF_3CH_2OH is endothermic by 34 kcal mol^{-1} for M = Li and by 26 kcal mol^{-1} for M = Na. Under FTICR conditions no reaction is observed between $H_3P_2O_7^-$ or $LiH_2P_2O_7^-$ and CF_3CH_2OH. The $[MH_2P_2O_7,CF_3CH_2OH]^-$ adducts are formed from all the other $MH_2P_2O_7^-$ ions, and the rate constants of adduct formation increase from Na to Rb owing to the lower acidity difference between $MH_3P_2O_7$ and 1,1,1-trifluoroethanol. However, the total efficiency does not exceed 1%. In view of its higher acidity (ΔH°_{acid} = 345.0 kcal mol^{-1}),[27] the clustering efficiency rises to 10% of the collision rate constant K_{ADO} with $(CF_3)_2CHOH$, which also reacts with $LiH_2P_2O_7^-$.

Molecular clusters are unique environments for investigating the gas-phase behavior of cluster components. The induced collisional activation of the $[MH_2P_2O_7,CF_3CH_2OH]^-$ and $[MH_2P_2O_7,(CF_3)_2CHOH]^-$ clusters formed directly in the ESI source of the TQ mass spectrometer revealed that the dissociation energy of these clusters is always lower than the energy needed to promote any of the processes between cluster components.

In principle, the fragmentation into $H_2PO_4^-$ ions could be indicative of the hydrolysis of pyrophosphate ions induced by proton transfer from the alcohol to the phosphate, followed by nucleophilic attack of the alkoxide anion on a P atom and breaking of the P-O-P bond. This mechanism was postulated by Beauchamp et al. for phosphorylation of the OH group of choline in the $[choline + triphosphate\text{-}2H]^-$, $[choline + triphosphate\text{-}3H + Na]^-$ clusters.[21]

However, in our case, the intensity of the $H_2PO_4^-$ fragment obtained from collisional activation of the $[MH_2P_2O_7,CF_3CH_2OH]^-$ and the $[MH_2P_2O_7,(CF_3)_2CHOH]^-$ clusters remains very low.

Moreover, the presence of this ion cannot be attributed to collisionally induced dissociation of the $MH_2P_2O_7^-$ ion, since it occurs at considerably lower collision energies. This evidence could be an indication of activation of pyrophosphate hydrolysis in the gas phase, although its very low intensity does not allow us to draw any final conclusions.

The reaction of $MH_2P_2O_7^-$ ions with $(CH_3)_3SiN_3$ yields ionic products derived from the addition of one or more $(CH_3)_3SiN_3$ molecule(s) followed by the loss of one HN_3 molecule.

Nucleophiles with a proton affinity lower than that of Cl^- ($\Delta H^\circ_{acid}(HCl)$ = 333.4 kcal mol^{-1}) react with $(CH_3)SiCl$ by addition/HCl elimination.[28,29] This reaction, analogous to the reaction of hydroxide ion with tetramethylsilane,[29] was also observed for singly charged phosphorylated oligonucleotides.[28] A pentacoordinate adduct arising from nucleophilic attack of an oxygen atom on the Si atom is probably involved, which decomposes by elimination of Cl^- ion and subsequent deprotonation of the incipient trimethylsilyldiphosphoric acid. The lower proton affinity of $MH_2P_2O_7^-$ ions (M = Li, Na) compared to N_3^- (343.9 kcal mol^{-1}) and entropic factors favor the elimination channel allowing stabilization of trimethylsilated species.

Conclusion

The gas-phase ion chemistry of polyphosphate species is practically unexplored, even though knowledge thereof could contribute to clarifying the factors that affect the stability and reactivity of these species in solution and may enhance the comprehension of enzymatic mechanisms involving phosphate esters. In this context, the results presented here are an important addition to our systematic investigation of the gas-phase properties of inorganic phosphates. In our previous study,[25] the gaseous $H_3P_2O_7^-$ ion derived from electrospray ionization of solutions containing $H_4P_2O_7$ was structurally characterized essentially as the linear pyrophosphate anion, a stable inorganic species strongly stabilized by two internal hydrogen bonds. The $H_3P_2O_7^- \rightarrow [H_3PO_4\cdots PO_3]^-$ isomerization, which proceeds through a proton shift to the bridging oxygen atom, induced by collisional activation, was computed to be endothermic by 18.1 kcal mol^{-1} with a barrier height of 36.9 kcal mol^{-1} at the CCSD(T)/6-31+G* level of theory.

Coordination of alkali metal ions affects chemical behavior of pyrophosphate in various ways. The activation barrier for the isomerization $MH_2P_2O_7^- \rightarrow [H_2PO_4\cdots M\cdots PO_3]^-$ was found to be comparable to that of the pyrophosphate anion and decreases on going from the $LiH_2P_2O_7^-$ to $NaH_2P_2O_7^-$. In addition, whereas dissociation of the cluster $[H_3PO_4\cdots PO_3]^-$ was computed to be endothermic by 36.5 kcal mol^{-1} at the CCSD(T) level of theory, dissociation of the $[H_2PO_4\cdots M\cdots PO_3]^-$ anions (M = Li and Na) was found to be exothermic and strongly dependent on the nature of the metal cation. Indeed, coordination of alkali metal ions influences the entire enthalpy of the isomerization process. Remarkably, the overall conversion of $MH_2P_2O_7^-$ to PO_3^- and MH_2PO_4 in the gas phase is exothermic by 3.9 and 14.9 kcal mol^{-1} for M = Li and M = Na, respectively.

The observed reactivity evidences the role played by the metal cation in allowing the nucleophile to be activated and correctly arranged. The $H_3P_2O_7^-$ ions were found to be inert toward several compounds, whereas the $MH_2P_2O_7^-$ ions showed interesting reactivity with species such as CF_3COOH and CF_3CH_2OH, even though no evidence of phosphorylation reactions was found.

Besides the specific interest in alkali metal coordination, the generalization of the results presented here and their extension from the gas phase to the active enzyme site could clarify the role played by noncovalent interactions between the phosphate group and metal cations or amino acid chain during enzymatic processes. For example, the coordination of $H_2P_2O_7^{2-}$ ions with M^+ ions having low charge-to-radius ratios, mimicking weak noncovalent interactions, increases the Coulombic repulsions between the phosphate negative charges and favours breaking of the P-O-P bond.

Experimental Section

Materials: $H_4P_2O_7$, $Na_4P_2O_7$, MOH, MNO_3 and all other chemicals were purchased from Sigma-Aldrich Ltd. and used as received.

Instrumentation: ESI-FTICR-MS experiments were performed with a Bruker BioApex 4.7 T FTICR mass spectrometer equipped with an Analytica of Brandford Electrospray Ionization Source. Samples were infused into a fused-silica capillary (i.d. 50 μm) at a flow rate of 130 $\mu L\,h^{-1}$, and the ions accumulated in a hexapole ion guide for 0.8 s. Typical ESI voltages for cylinder, capillary and end plates were 3000, 4000, and 4300 V, respectively. The capillary exit and skimmer voltages were set to −60 and −10 V, respectively, and hexapole d.c. offset was 0.7 V.

Triple quadrupole mass spectra were recorded on a TSQ 700 mass spectrometer from Finnigan Ltd operating in the negative-ion mode.

Methods: The $MH_2P_2O_7^-$ ions were obtained by electrospray ionization of solutions of $H_4P_2O_7$ and a source of M^+ ions (M salts or MOH) in acetonitrile/water (1/1) or from solutions of $Na_4P_2O_7$ in acetonitrile/water (1/1). ESI solutions were prepared daily at a concentration of 10^{-4} M and used immediately for analysis. In the FTICR experiments, the $MH_2P_2O_7^-$ ions were transferred into the resonance cell (25 °C) and isolated by broad-band and "single-shot" ejection pulses. After thermalization by collisions with neutral reactants for delay times of 1–2 s or with Ar introduced into the cell through a pulsed valve, the ions were re-isolated by single shots and allowed to react with reagents in the cell. The pressure of the neutral reactants, which ranged from 10^{-8} to 10^{-7} mbar, was measured by a Bayard–Alpert ionization gauge, calibrated by using as reference the known rate coefficient of the reaction $CH_4 + CH_4^+ \rightarrow CH_5^+ + CH_3$. The readings were corrected for the relative sensitivity to the various gases used according to a standard method.[30] The pseudo-first-order rate constants were obtained by plotting the $\lg(I_t/I_{t=0})$ of $[MH_2P_2O_7]^-$ as a function of the reaction time. Then the bimolecular rate constants were determined from the number density of the neutral molecules, deduced in turn from the pressure of the gas. Average dipole orientation (ADO) collision rate constants k_{ADO} were calculated as described by Su and Bowers.[31] Reaction efficiencies (RE) are the ratio of the experimental rate constants k_{exp} to the collision rate constants k_{ADO}. The absolute uncertainty of each rate constant is estimated to be 30%.

In the triple quadrupole (TQ) mass spectrometric experiments, the $MH_2P_2O_7^-$ ions were isolated by the first quadrupole (Q1) and driven into the collision cell, actually an RF-only hexapole, containing the neutral reagent at a pressure of up to 1 mtorr. Collisionally activated dissociation (CAD) experiments were performed with Ar as target gas at a pressure of $(1–5)\times10^{-5}$ Torr and collision energies ranging from 0 to 50 eV (laboratory frame). Laboratory (lab) ion energies are converted to energies in the center-of-mass frame (cm) by using the formula $E_{cm} = E_{lab}m(m+M)$, where m and M are neutral Ar and ionic reactants, respectively. The charged products were analyzed with the third quadrupole, scanned at a frequency of 150 $amu\,s^{-1}$.

Computational details: DFT with the hybrid[32] B3LYP functional[33] was used to localize the stationary points on the investigated potential energy surface. This functional is based on Becke's three-parameter functional including a Hartree–Fock contribution and comprises the nonlocal correction for the exchange potential proposed by Becke together with the nonlocal correction for the correlation energy provided by the functional of Lee, Yang and Parr. The 6-31+G* basis set[34] was used for H, O, and P. The same basis set was implemented for Li, whereas Na, K, Rb, and Cs were described by using a LANL2DZ basis with the corresponding relativistic pseudopotential.[35] For simplicity, these calculations are also referred to as B3LYP/6-31+G*. All calculations were carried out with the Gaussian 98 suite of programs.[36]

The nature (minima or saddle points) of the critical points investigated along the potential energy surfaces was determined by computing the harmonic frequencies at the same level of theory. Thermochemical calculations were carried out at 298.15 K and 1 atm by adding the zero-point correction and the thermal corrections to the calculated B3LYP energies. The absolute entropies were evaluated by using standard statistical-mechanical procedures from scaled harmonic frequencies and moments of inertia relative to the optimized geometries.

Acknowledgement

Financial support from the Italian Ministero dell'Università e della Ricerca Scientifica e Tecnologica (MURST) is gratefully acknowledged.

[1] R. Wolfenden, M. J. Snider, *Acc. Chem. Res.* **2001**, *31*, 938–945.
[2] I. S. Kulaev, V. M. Vagabov, T. V. Kulakovskaya in *The Biochemistry of Inorganic Polyphosphates*, 2nd ed., Wiley, New York, **2004**, pp. 65–87.
[3] D. E. Wilcox, *Chem. Rev.* **1996**, *96*, 2435–2458.
[4] A. G. Cassano, V. E. Anderson, M. E. Harris, *Biochemistry* **2004**, *43*, 10547–10559, and references therein.
[5] a) M. Padovani, N. H. Williams, P. Wyman, *J. Phys. Org. Chem.* **2004**, *17*, 472–477 and references therein; b) T. Humphry, M. Forconi, N. H. Williams, A. C. Hengge, *J. Am. Chem. Soc.* **2004**, *126*, 11864–11869 and references therein.
[6] C. Vichard, T. A. *Kaden, Inorg. Chim. Acta* **2004**, *357*, 2285–2293.
[7] R. Wolfendeng, F. Zhao, *J. Am. Chem. Soc.* **2004**, *126*, 8646–8647.
[8] E. Franzini, P. Fantucci, L. De Gioia, *J. Mol. Catal. A* **2003**, *204–205*, 409–417.
[9] R. A. Torres, F. Himo, T. C. Bruice, L. Noodlemann, T. Lovell, *J. Am. Chem. Soc.* **2003**, *125*, 9861–9867.
[10] E. Buncel, R. Nagelkerke, G. R. J. Thatcher, *Can. J. Chem.* **2003**, *81*, 53–63.
[11] W. J. McCarthy, L. Adamowicz, H. Saint-Martin, I. Ortega-Blake, *Rev. Soc. Quim. Mex.* **2002**, *46*, 145–158.
[12] H. Saint-Martin, L. E. Vicent, *J. Phys. Chem. A* **1999**, *103*, 6862–6872.
[13] W. J. McCarthy, D. M. A. Smith, L. Adamowicz, H. Saint-Martin, I. Ortega-Blake, *J. Am. Chem. Soc.* **1998**, *120*, 6113–6120.
[14] H. Saint-Martin, L. E. Ruiz-Vicent, A. Ramìrez-Solìs, I. Ortega-Blake, *J. Am. Chem. Soc.* **1996**, *118*, 12167–12173.
[15] a) B. Ma, C. Meredith, H. F. Schaefer III, *J. Phys. Chem.* **1995**, *99*, 3815–3822; b) B. Ma, C. Meredith, H. F. Schaefer III, *J. Phys. Chem.* **1994**, *98*, 8216–8223.
[16] a) A. T. Blades, Y. Ho, P. J. Kebarle, *J. Phys. Chem.* **1996**, *100*, 2443–2446; b) A. T. Blades, Y. Ho, P. J. Kebarle, *J. Am. Chem. Soc.* **1996**, *118*, 196–201.
[17] X.-B. Wang, E. R. Vorpagel, X. Yang, L.-S. Wang, *J. Phys. Chem. A* **2001**, *105*, 10468–10474.
[18] B. K. Choi, D. M. Hercules, M. Houalla, *Anal. Chem.* **2000**, *72*, 5087–5091.
[19] For example, see: a) J. Jankowski, P. Grosse-Huttmann, W. Zidek, H. Schulter, *Rapid Commun. Mass Spectrom.* **2003**, *17*, 1189–1194; b) F.-F. Hsu, J. Turk, M. L. Gross, *J. Mass Spectrom.* **2003**, *38*, 447–457.
[20] a) R. C. Lum, J. J. Grabowski, *J. Am. Chem. Soc.* **1992**, *114*, 8619–8627; b) R. C. Lum, J. J. Grabowski, *J. Am. Chem. Soc.* **1993**, *115*, 7823–7832.
[21] H. A. Cox, R. Hodyss, J. L. Beauchamp, *J. Am. Chem. Soc.* **2005**, *127*, 4084–4090 and references therein.
[22] H. Saint-Martin, I. Ortega-Blake, A. Les, L. Adamowicz, *Biochim. Biophys. Acta* **1991**, *1080*, 205–214.
[23] M. E. Colvin, E. Evleth, Y. Akacem, *J. Am. Chem. Soc.* **1995**, *117*, 4357–4362.
[24] H. Saint-Martin, I. Ortega-Blake, A. Les, L. Adamowicz, *Biochim. Biophys. Acta* **1994**, *1207*, 12–23.
[25] F. Pepi, A. Ricci, M. Rosi, M. Di Stefano, *Chem. Eur. J.* **2004**, *10*, 840–850.
[26] F. Pepi, A. Ricci, M. Rosi, M. Di Stefano, *Chem. Eur. J.* **2004**, *10*, 5706–5716.
[27] NIST Chemistry WebBook, NIST standard Reference Database No. 69, Feb. 2000 release; data collection of the National Institute of

Standards and Technology to be found under http://webbook.nist.gov.
[28] R. A. J. O'Hair, S. C. McLuckey, *Int. J. Mass Spectrom. Ion Processes* **1997**, *162*, 183–202.
[29] J. C. Sheldon, R. N. Hayes, J. H. Bowie, C. H. DePuy, *J. Chem. Soc. Perkin Trans. 2*, **1987**, 275–280.
[30] J. E. Bartmess, R. M. Georgiadis, *Vacuum* **1983**, *33*, 149–153.
[31] T. Su, M. T. Bowers, *Int. J. Mass Spectrom. Ion Phys.* **1973**, *12*, 347.
[32] A. D. Becke, *J. Chem. Phys.* **1993**, *98*, 5648–5652.
[33] a) A. D. Becke, *Phys. Rev. A* **1988**, *38*, 3098–3100; b) C. Lee, W. Yang, G. G. Parr, *Phys. Rev. B* **1988**, *37*, 785–789.
[34] J. C. Rienstra-Kiracofe, G. S. Tschumper, H. F. Schaefer III, *Chem. Rev.* **2002**, *102*, 231–282.
[35] a) P. J. Hay, W. R. Wadt, *J. Chem. Phys.* **1985**, *82*, 270–283; b) W. R. Wadt, P. J. Hay, *J. Chem. Phys.* **1985**, *82*, 284–298; c) P. J. Hay, W. R. Wadt, *J. Chem. Phys.* **1985**, *82*, 299–310.
[36] Gaussian 98 (Revision A.1), M. J. Frisch, G. W. Trucks, H. B. Schlegel, G. E. Scuseria, M. A. Robb, J. R. Cheeseman, V. G. Zakrzewski, J. A. Montgomery, R. E. Stratmann, J. C. Burant, S. Dapprich, J. M. Millam, A. D. Daniels, K. N. Kudin, M. C. Strani, O. Farkas, J. Tomasi, V. Barone, M. Cossi, R. Cammi, B. Mennucci, C. Pomelli, C. Adamo, S. Clifford, J. Ochterski, G. A. Petersson, P. Y. Ayala, Q. Cui, K. Morokuma, D. K. Malick, A. D. Rabuck, K. Raghavachari, J. B. Foresman, J. Cioslowski, J. V. Ortiz, B. B. Stefanov, G. Liu, A. Liashenko, P. Piskorz, I. Komaromi, R. Gomperts, R. L. Martin, D. J. Fox, T. Keith, M. A. Al-Laham, C. Y. Peng, A. Nanayakkara, C. Gonzalez, M. Challacombe, P. M. W. Gill, B. G. Johnson, W. Chen, M. W. Wong, J. L. Andrei, M. Head-Gordon, E. S. Replogle, J. A. Pople, Gaussian, Inc., Pittsburgh, PA, **1998**.

Received: June 23, 2005
Revised: November 2, 2005
Published online: January 17, 2006

